

CHAPTER-2 EXPERIMENTAL

2.1 Materials

2.1.1 Composition and dimensions of used Mild steel sample

The mild steel (MS) strips of 2 cm x 2.5 cm x 0.025 and 8 cm x 1 cm x 0.025 cm dimensions were used for weight loss as well as for electrochemical study. The composition of MS is given as:

C	P	Si	Mn	Cr	Cu	Al	Ni	Fe
0.17%	0.46%	0.026%	0.050%	0.012%	0.135%	0.023%	0.05%	Balance

2.1.2 Test solution

The 1 M HCl test solution was prepared by diluting analytical grade 37% HCl with double distilled water.

2.1.3 Inhibitors

Thirteen compounds were synthesized in the laboratory by the previously reported methods, characterised and evaluated as corrosion inhibitors for MS in 1 M HCl. These inhibitors are divided into four sections as given below:

(A) Nicotinonitrile derivatives (ATN and AMN)

(1) 2-amino-6-phenyl-4-(*p*-tolyl)nicotinonitriles (ATN)

(2) 2-amino-4-(4-methoxyphenyl)-6-phenylnicotinonitrile (AMN)

(B) Naphthyridine Derivatives (N-1, N-2 and N-3)

(1) 5-amino-9-hydroxy-2-phenylchromeno[4,3,2-de][1,6]naphthyridine-4 carbonitrile (N-1)

(2) 5-amino-9-hydroxy-2-(p-tolyl)chromeno[4,3,2-de][1,6]naphthyridine-4- carbonitrile (N-2)

(3) 5-amino-9-hydroxy-2-(4-methoxyphenyl)chromeno[4,3,2-de][1,6]naphthyridine-4-carbonitrile (N-3)

(C) Quinoline derivatives (Q-1, Q-2, Q-3 and Q-4)

(1) 2-amino-7-hydroxy-4-phenyl-1,4-dihydroquinoline-3-carbonitrile (Q-1)

(2) 2-amino-7-hydroxy-4-(p-tolyl)-1,4 dihydroquinoline-3-carbonitrile (Q-2)

(3) 2-amino-7-hydroxy-4-(4-methoxyphenyl)-1,4 dihydroquinoline-3 carbonitrile (Q-3)

(4) 2-amino-4-(4-(dimethylamino)phenyl)-7-hydroxy-1,4-dihydroquinoline-3- carbonitrile (Q-4)

(D) Thiopyrimidine derivatives (TP-1, TP-2, TP-3 and TP-4)

(1) 5-cyano-6-phenyl-2-thioxo-2,3-dihydropyrimidin-4(1H)-one (TP-1)

(2) 5-cyano-2-thioxo-6-(p-tolyl)-2,3 dihydropyrimidin-4(1H)-one (TP-2)

(3) 5-cyano-6-(4-methoxyphenyl)-2-thioxo-2,3-dihydropyrimidin-4(1H)-one (TP-3)

(4) 6-(4-(dimethylamino)phenyl)-5-cyano-2-thioxo-2,3-dihydropyrimidin-4(1H)- one (TP-4)

2.2 Synthesis of inhibitors

(A) Synthesis of Nicotinonitriles derivatives [Safari *et al.* (2012)]

A mixture of malononitrile, aldehydes, acetophenone, and ammonium acetate was added in water. The reacting solution mixture was placed in ultrasound and

irradiated as reported in the literature. Completion of the reaction was monitored by TLC. Upon completion of the reaction, the solid product was filtered washed with water, dried and recrystallized from ethanol.

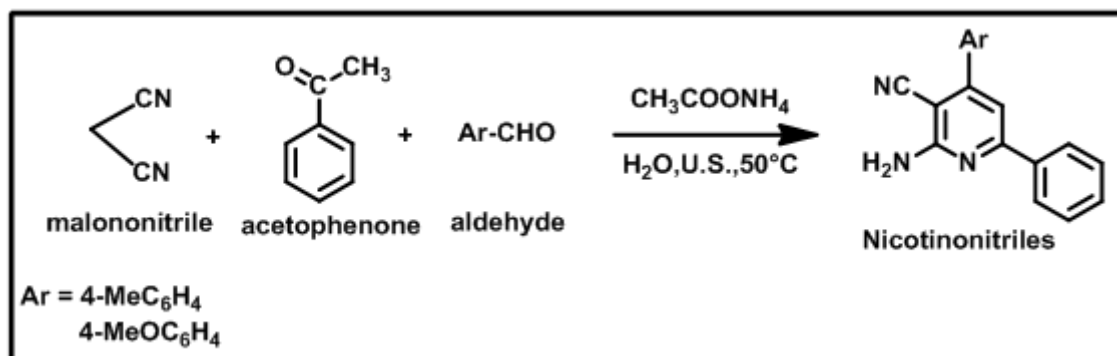


Figure 2.1.1 Synthesis of Nicotinonitrile derivatives.

Table 2.1.1 The molecular structure and IUPAC name of synthesized Nicotinonitrile derivatives.

IUPAC Name	Molecular Structure	Analytical Data
2-amino-6-phenyl-4-(<i>p</i> -tolyl)nicotinonitrile (ATN)		¹ HNMR (500 MHz, DMSO): 9.23, 7.75-7.66, 7.61, 7.49-7.46, 7.40, 6.81, 2.48, IR (KBr) cm ⁻¹ : 3370, 3350, 3230, 2224, 1662.
2-amino-4-(4-methoxyphenyl)-6-phenylnicotinonitrile (AMN)		¹ HNMR (500 MHz, DMSO): 8.15-8.13, 7.64, 7.49-7.48, 7.23, 7.12, 7.2, 3.80, IR (KBr) cm ⁻¹ : 3460, 3407, 3180, 2210, 1635.

(B) Synthesis of Naphthyridine derivatives [Wu *et al.* (2010)]

A mixture of aromatic aldehydes, 2,4-dihydroxy acetophenone, malononitrile and silica gel was stirred in water at 80 °C. After completion of the reaction the obtained product was filtered and dried. The product was recrystallized from ethanol.

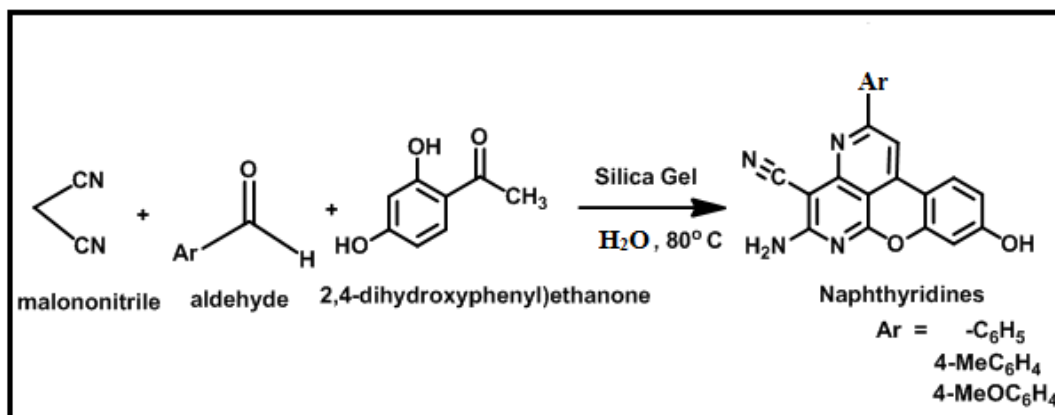


Figure 2.1.2 Synthesis of Naphthyridine derivatives.

Table 2.1.2 The molecular structure and IUPAC name of synthesized Naphthyridine derivatives.

IUPAC Name	Molecular Structure	Analytical Data
5-amino-9-hydroxy-2-phenylchromeno[4,3,2-de][1,6]naphthyridine-4-carbonitrile (N-1)		¹ HNMR (500 MHz, DMSO): 11.35, 7.89-7.88, 7.76, 7.63-7.51, 6.35-6.34, 6.35, IR (KBr) cm ⁻¹ : 3480, 3293, 3163, 2209, 1640.
5-amino-9-hydroxy-2-(<i>p</i> -tolyl)chromeno[4,3,2de][1,6]naphthyridine-4-carbonitrile (N-2)		¹ HNMR (500 MHz, DMSO): 11.33, 7.80-7.78, 7.70, 7.32-7.31, 7.24, 6.33, 2.43, IR (KBr) cm ⁻¹ : 3487, 3289, 3161, 2206, 1636.
5-amino-9-hydroxy-2-(4-methoxyphenyl)chromeno[4,3,2de][1,6]naphthyridine-4-carbonitrile (N-3)		¹ HNMR (500 MHz, DMSO): 11.31, 7.90-7.88, 7.63, 7.24, 7.00-6.98, 6.35, 3.89, IR (KBr) cm ⁻¹ : 3455, 3381, 3290, 3165, 2209, 1641.

(C) Synthesis of Quinoline derivatives [Javanshir and Safari (2010)]

A mixture of aldehydes, resorcinol, malononitrile and ammonium acetate in water was irradiated by microwave as reported. After completion of reaction the deposited solid was collected by filtration and washed with water then dried. The crude product was recrystallized from ethanol.

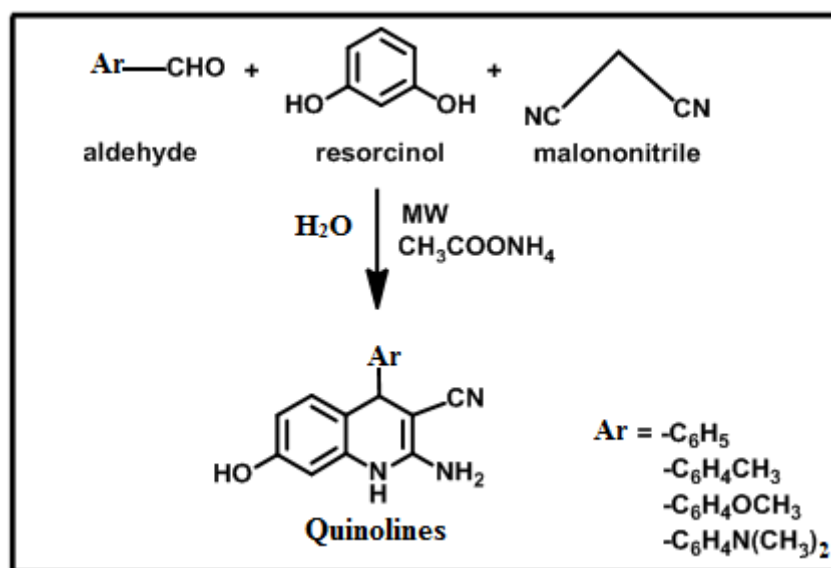
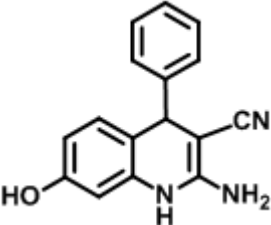
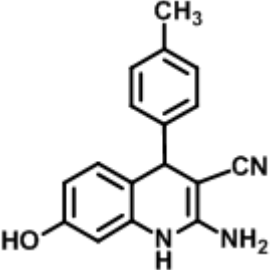
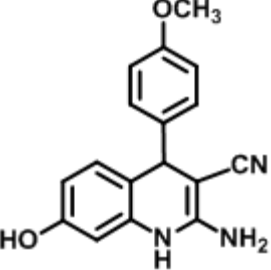
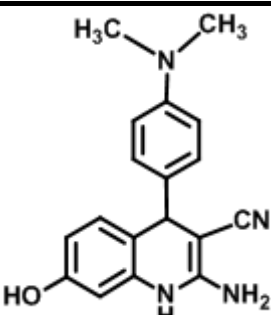


Figure 2.1.3 Synthesis of Quinoline derivatives.

Table 2.1.3 The molecular structure and IUPAC name of synthesized Quinoline derivatives.

Inhibitors	Molecular Structures	Analytical Data
2-amino-7-hydroxy-4-phenyl-1,4-dihydroquinoline-3-carbonitrile (Q-1)		¹ HNMR (500 MHz, DMSO): 4.60, 6.63, 6.72, 6.75, 6.83, 7.18-7.23, 7.93, 9.73, IR (cm ⁻¹): 3430, 3345, 3210, 2223, 1640, 1581.
2-amino-7-hydroxy-4-(<i>p</i> -tolyl)-1,4-dihydroquinoline-3-carbonitrile (Q-2)		¹ HNMR (500 MHz, DMSO): 2.53, 4.59, 6.58, 6.64, 6.67, 6.73, 7.12-7.21, 7.91, 9.69, IR (cm ⁻¹): 3430, 3343, 3208, 2220, 1640, 1577.
2-amino-7-hydroxy-4-(4-methoxyphenyl)-1,4-dihydroquinoline-3-carbonitrile (Q-3)		¹ HNMR (500 MHz, DMSO): 2.65, 4.54, 6.48, 6.57, 6.62, 6.71, 7.09-7.17, 7.76, 9.63, IR (cm ⁻¹): 3425, 3340, 3206, 2218, 1639, 1556.
2-amino-4-(4-(dimethylamino)phenyl)-7-hydroxy-1,4-dihydroquinoline-3-carbonitrile (Q-4)		¹ HNMR (500 MHz, DMSO): 2.61, 4.43, 6.45, 6.49, 6.53, 6.64, 7.03-7.12, 7.73, 9.57, IR (cm ⁻¹): 3421, 3335, 3203, 2219, 1637, 1545.

(D) Synthesis of Thiopyrimidine derivatives [Sahoo *et al.* (2013)]

A mixture of aldehydes, ethylcyanoacetate, thiourea and potassium carbonate in ethanol was irradiated by microwave. The obtained product was washed with cold water, dried and recrystallized from ethanol.

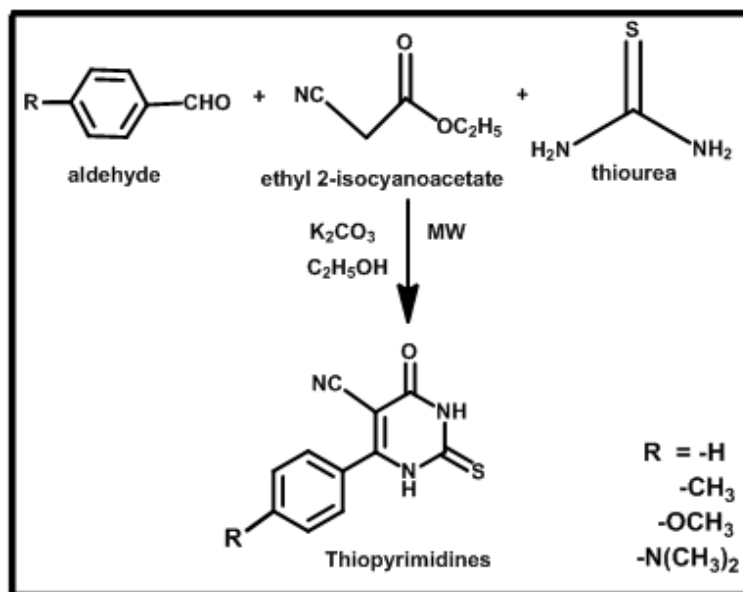
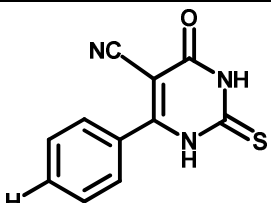
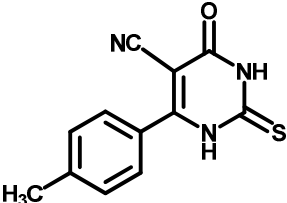
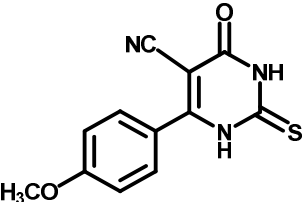
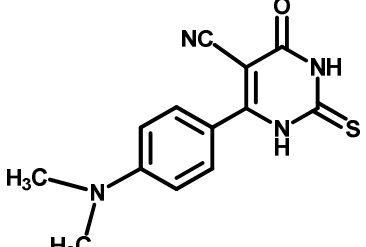


Figure 2.1.4 Synthesis of Thiopyrimidine derivatives.

Table 2.1.4 The molecular structure and IUPAC name of synthesized Thiopyrimidine derivatives.

Inhibitors	Molecular Structures	
5-cyano-6-phenyl-2-thioxo-2,3-dihydropyrimidin-4(1H)-one (TP-1)		¹ HNMR (300 MHz, DMSO): 8.31, 7.96-7.26, 7.07, IR (cm ⁻¹): 3525, 3150, 2235, 1795, 1640
5-cyano-2-thioxo-6-(<i>p</i> -tolyl)-2,3-dihydropyrimidin-4(1H)-one (TP-2)		¹ HNMR (300 MHz, DMSO): 8.30, 7.84, 7.77-7.03, 2.37, IR (cm ⁻¹): 3490, 3135, 2220, 1760, 1625
5-cyano-6-(4-methoxyphenyl)-2-thioxo-2,3-dihydropyrimidin-4(1H)-one (TP-3)		¹ HNMR (300 MHz, DMSO): 8.32, 8.11-8.80, 7.18-7.15, 7.0, IR (cm ⁻¹): 3430, 3090, 2210, 1745, 1610
6-(4-(dimethylamino)phenyl)-5-cyano-2-thioxo-2,3-dihydropyrimidin-4(1H)-one (TP-4)		¹ HNMR (300 MHz, DMSO): 8.11, 7.95-7.98, 7.09, 6.28-6.85, 3.09, IR (cm ⁻¹): 3410, 3030, 2198, 1693, 1590.

2.3 Equipments and techniques used

2.3.1 Weight loss method for determination of corrosion rate

Weight loss experiments were performed using MS coupons having following dimension 2.5 cm × 2.0 cm × 0.025 cm. These MS samples were abraded by using emery paper (600-1200 grade) then washed with double distilled water and finally dried. The surface area of the MS samples was measured by the following equation [ASTM (1990)],

$$A = 2 (lb + lt + bt - \pi r^2 + \pi rt) \quad (2.1)$$

where, l represent length, b width, t thickness of the sample in cm and r is the radius of the mounting hole.

The weight loss experiment was conducted by correctly weighed MS samples and immerses them with the help of thread in a 100 ml conical flask in absence and presence of used inhibitors for 3 h. The experiment was performed in varying concentration and solution temperature. The weight loss experiments were performed in triplicate to ensure the reproducibility for observations. After, the completion time, these MS samples were taken out washed with water then dried and weighed. By calculating the difference in weight loss before and after immersion time, following parameters can be calculated such as corrosion rate, C_r inhibition efficiency, $\eta\%$ and surface coverage, θ using following equations [ASTM (1987)],

$$C_r(\text{mm/y}) = \frac{87.6W}{atD} \quad (2.2)$$

$$\eta\% = \frac{C_r - {}^iC_r}{C_r} \times 100 \quad (2.3)$$

$$\theta = \frac{C_r - {}^iC_r}{C_r} \quad (2.4)$$

where W is the average weight loss, a is total surface area of MS specimen, t is the immersion time (3 h) and D is the density of MS in (gcm^{-3}). In equation (2.3) C_r and iC_r is the corrosion rates of MS in the absence and presence of the inhibitors respectively.

2.3.2 Electrochemical measurements

The electrochemical experiments: Electrochemical impedance spectroscopy (EIS) and Potentiodynamic polarization were conducted by using a three-electrode cell system connected to the Potentiostat/Galvanostat G300-45050 (Gamry Instruments Inc., USA). Gamry Echem Analyst 5.50 software package was used for data analyses, and fitting [ASTM (1991)]. In this three-cell system the MS strips of 8 cm x 1 cm x 0.025 cm dimension with exposed area of 1 cm² is used as working electrode. The graphite and saturated calomel electrodes (SCE) are used as auxiliary and reference electrodes correspondingly. All experiments were carried out at 308 K. The electrochemical experiments were performed after immersing the MS strips for 30 min in the respective testing solutions.

2.3.2.1 Electrochemical impedance spectroscopy: EIS measurements were carried out in a frequency range from 100 kHz to 0.01 Hz, with amplitude of 10 mV AC signal using three electrode systems. The impedance parameters like R_{ct} , C_{dl} were analyzed by using equivalent circuit model for data fitting containing R_s (solution resistance), CPE (constant-phase element) parallel to the R_{ct} (charge-transfer resistance). The CPE is used in the model for accurately determining the depressed capacitive semi-circle Nyquist loops. This appearance of the loops is attributed due to the surface roughness, frequency dispersion, relaxation and porous surface of MS. The impedance function of the CPE is expressed by the equation [Ahamad and Quraishi (2010)],

$$Z_{CPE} = Y^{-1}(j\omega)^{-n} \quad (2.5)$$

where Y is the amplitude of CPE, j is the square root of -1, ω is angular frequency and n is the phase shift.

The R_{ct} was obtained by calculating the difference in impedance at lower and higher frequencies which is attributed due to the resistance developed between outer Helmholtz planes of metal surface. The corrosion inhibition efficiency ($\eta\%$) and corresponding double layer capacitance (C_{dl}) was calculated by the following equations [Ahamad *et al.* (2010)],

$$\eta\% = \left(1 - \frac{R_{ct}}{R_{ct(i)}}\right) \times 100 \quad (2.6)$$

where R_{ct} and $R_{ct(i)}$ are the values of charge transfer resistance in the absence and presence of inhibitors respectively.

$$C_{dl} = \frac{Y^o \omega^{n-1}}{\sin(n(\pi / 2))} \quad (2.7)$$

where, ω is angular frequency and n is the phase shift, which depicts the heterogeneity or surface roughness for MS.

2.3.2.2 Potentiodynamic polarization: The Potentiodynamic polarization analysis were performed by sweeping the electrode potential range from -0.25 V to $+0.25$ V versus open circuit potential at a scan rate of 1.0 mVs^{-1} scan rate. The parameters like corrosion potential, E_{corr} corrosion current density, i_{corr} were calculated after analysis of the obtained data. The inhibition efficiencies were calculated from i_{corr} values using the following equation [Shukla and Quraishi (2009)],

$$\eta\% = \left(1 - \frac{i_{\text{corr}}}{i_{\text{corr}}}\right) \times 100 \quad (2.8)$$

where, i_{corr} and i_{corr} shows the corrosion current densities in the absence and presence of inhibitors respectively, in 1 M HCl.

2.4 Thermodynamic parameters

2.4.1 Activation energy: The effect of temperature on activation energy for MS is calculated by using Arrhenius equation [Singh and Quraishi (2010)],

$$\ln(C_r) = \frac{-E_a}{RT} + A \quad (2.9)$$

where, E_a is the activation energy for corrosion of MS, R is the gas constant, A the Arrhenius pre-exponential factor and T is the absolute temperature. A plot between the corrosion rate and temperature ($\log C_r$ vs $1000/T$) gives a straight line. The activation energy in absence and presence of inhibitor is determined by the slope obtained from the plot.

2.4.2 Free energy of adsorption: The interaction between inhibitor molecules and MS surface can be better understood by adsorption isotherm. The adsorption of inhibitor molecules on the corroding MS surface not attains the complete equilibrium. When retardation in corrosion rate occurs in presence of inhibitor then a quasi equilibrium state occurs through the adsorption process. The nature of quasi equilibrium adsorption of inhibitors can be investigated using appropriate adsorption isotherm. Different adsorption isotherms including Langmuir, Temkin and Freundlich isotherms used to fit the observed experimental results are given as [Yadav and Quraishi (2012) (a)],

$$\text{Temkin isotherm } \exp(f \cdot \theta) = K_{\text{ads}} \cdot C \quad (2.10)$$

$$\text{Freundlich isotherm } \theta = K_{\text{ads}} \cdot C \quad (2.11)$$

$$\text{Langmuir isotherm } (\theta/1-\theta) = K_{\text{ads}} \cdot C \quad (2.12)$$

where, K_{ads} designates the equilibrium constant for adsorption process, C is the concentration of inhibitor and f is energetic inhomogeneities. The free energy of adsorption can be calculate by the following equation [Yadav and Quraishi (2012) (a)],

$$\Delta G_{\text{ads}} = -RT \ln(55.5K_{\text{ads}}) \quad (2.13)$$

where, T represent the absolute temperature and R stands for the gas constant. In this equation 55.5 is the concentration of water in solution in mol L⁻¹.

2.5 Scanning electron microscopy (SEM)

Surface morphology of MS in absence and presence of inhibitors is analysed by SEM. The 3 h immersed without and with inhibitor of MS samples having following dimensions 2.5 cm × 2.0 cm × 0.025 cm was cut into 1 cm² size for surface analysis. These prepared samples were analysed by using SEM model Supra 40, Carl Zeiss, Germany at 500 x magnifications.

2.6 Atomic force microscopy (AFM)

AFM is another method for surface analysis. The MS surface in absence and presence of inhibitor was analysed by using Bruker Dimension Icon SPM with tapping mode in Air, RTESPA probe; $k = 40$ N/m and $f_0 = 302$ kHz, at 10 μ m.

2.7 X-ray photoelectron spectroscopy (XPS)

The XPS spectra of inhibitor treated MS sample were recorded by using X-Ray Photoelectron Spectroscopy (AMICUS, Kratos Analytical, and Shimadzu, U.K.). The quantification of outer adsorbed inhibitor film and spectral simulation of the observed experimental peaks were achieved by using XPS peak fit 41 software.

2.8 Quantum chemical calculations

The Quantum chemical measurements were performed using the density functional theory (DFT) for the studied compounds. The Becke three-parameter hybrid functional along with Lee-Yang-Paar correlation functional (B3LYP) used in DFT [Becke (1993)], [Becke (1998)], [Lee *et al.* (1998)]. For all the calculations, the basis set 6-31+G (d, p) was selected. This computational study was carried out by using the Gaussian 09, software (Revision D.01) for Windows [Frisch *et al.* (2009)]. The effects of water on the geometry and electronic parameters were modelled using the integral equation formalism polarisable continuum model (IEFPCM) implemented in Gaussian 09. The studied compounds were first optimized and confirmed to correspond in its true energy minima by the absence of the imaginary frequency in the computed vibrational frequencies. The obtained quantum chemical parameters were explicated on the basis of their electronic parameters and also the most stable state of molecules conformation. The Frontier molecular orbitals (FMO), that is, the highest occupied molecular orbital energy (E_{HOMO}) and the lowest unoccupied molecular energy (E_{LUMO}) were calculated. Likewise the energy gap (ΔE), global electronegativity (χ), and fraction of electron moved from inhibitor to metal atom were calculated by the following equations [Martinez (2003)], [Olasunkanmi *et al.* (2015)],

$$\Delta E = E_{LUMO} - E_{HOMO} \quad (2.14)$$

$$\chi = -\frac{1}{2}(E_{LUMO} + E_{HOMO}) \quad (2.15)$$

$$\Delta N = \frac{\chi_{Fe} - \chi_{inh}}{2(\eta_{Fe} + \eta_{inh})} \quad (2.16)$$

where χ_{Fe} and η_{inh} respectively represent the electronegativity and hardness of iron and inhibitor.

The electronegativity 7 eV/mol value is used for χ_{Fe} , and hardness for η_{Fe} was taken as 0 eV/mol for bulk Fe atom based on the Pearson's electronegativity scale [Pearson (1998)].

The global hardness (η) and softness (σ) are calculated according to following equations,

$$\eta = \frac{E_{\text{HOMO}} - E_{\text{LUMO}}}{2} \quad (2.17)$$

$$\sigma = \frac{1}{\eta} \quad (2.18)$$

The calculated parameters like global hardness (η) and softness (σ) represent the reactivity of the molecule towards bond formation with metal [Abd El-Lateef (2015)].

The Fukui functions f^+ and f^- represent the local reactivity indices. By these parameters the susceptibility of active atomic sites of inhibitor molecules can be known for the electrophilic and nucleophilic attacks [Gomez *et al.* (2006)], [Yan *et al.* (2013)]. The approach of the atom condensed Fukui functions with using Mulliken population analysis (MPA) and the finite difference (FD) approximations was introduced by Yang and Mortier [Yang and Mortier (1986)], and recently employed in another study were calculated as,

$$f_k^+ = \rho_{k(N+1)}(r) - \rho_{k(N)}(r) \quad (2.19)$$

$$f_k^- = \rho_{k(N)}(r) - \rho_{k(N-1)}(r) \quad (2.20)$$

where f_k^+ and f_k^- stand for the electrophilic and nucleophilic Fukui indices, that is condensed with atom the k and $\rho_{k(N+1)}$, $\rho_{k(N)}$, $\rho_{k(N-1)}$ represent the electron densities of

the (N+1)-, (N)- and (N-1)- electron systems accordingly, approximated based on Mulliken gross charges. The Multiwfn software was used to visualize the electron density surfaces of f_k^+ and f_k^- [Lu and Chen (2012) (a)], [Lu and Chen (2012) (b)].

2.9 Monte Carlo simulation

Monte Carlo simulations were carried out to model the mode of adsorption of the studied inhibitor molecules on iron surface. The adsorption locator code implemented in the Material Studio 7.0 software from Biovia-Accelrys Inc. USA was adopted to compute the adsorption energy of the interaction between the inhibitor molecules and clean iron surface. The universal force field (UFF) was used in the entire simulation process for the optimization of the structures. Fe (110) crystal surface was selected for this simulation and to represent MS because it is the most stable surface. The Fe (110) surface was cleaved with a thickness of 5 Å. Then this cleaved plane was just enlarged to a (10 × 10) super cell. After that a vacuum slab of 30 Å thicknesses was built over the Fe (110) plane. The studied inhibitor molecules were used for the simulations in each case. The simulated annealing procedure adopted in this study uses the Monte Carlo method to determine the adsorption energy of the adsorbate substrate. During the simulated annealing, the adsorbate is heated and then cooled very slowly so that conformational changes taking place will lead to a local minimum being located. The process was repeated several times until very closely related, low energy conformations were obtained. Extensive literature about the Monte Carlo simulation can be found elsewhere [Madhankumar *et al.* (2014)], [Kumar *et al.* (2015)].